



Influence of Low-Frequency Vibration Acceleration on the Permeability of Low Permeable Porous Media During Water Flooding

Liming Zheng^{1,2(✉)}, Wenhao Cui³, Jing Liu², and Lei Zhang⁴

¹ College of Vehicles and Energy in Yanshan University, 066004, Qinhuangdao, China

upczlm@sina.cn

² College of Petroleum Engineering in China University of Petroleum(East China), 266580, Qingdao, China

³ Oil & Gas Technology Research Institute in Changqing Oil Company, CNPC, 710018, Xi'an, China

⁴ Department of Petroleum Engineering in China University of Geosciences, 430000, Wuhan, China

Abstract. Seismic production technology utilized physical wave field to stimulate the reservoir. Though this technology was applied once in the oil fields, the mechanisms were not analyzed comprehensively. Influence of low-frequency vibration acceleration instead of vibration frequency on rock properties of low permeable rock during water flooding was studied thereby. The variations of absolute or relative permeability were talked in detail. With introduction of four relative permeability models, coefficients of the models were matched and the change of pore size of rock under low-frequency vibration was discussed indirectly. It was found that, besides the vibration frequency, the vibration acceleration had also affected the properties of low permeable rock during water flooding. The absolute permeability, which decreased gradually due to stress sensitivity, had been retrieved partly by vibration. When the vibration acceleration was chosen properly, the relative permeability of water phase could be decreased and the relative permeability of oil phase could be enhanced. Because of the improved hydrophilicity of rock by vibration, violent

Copyright 2018 Shaanxi Petroleum Society

This paper was prepared for presentation at the 2018 International Field Exploration and Development Conference in Xi'an, China September 18–20, 2018.

This paper was selected for presentation by the IFEDC Committee following review of information contained in an abstract submitted by the author(s). Contents of the paper, as presented, have not been reviewed by the IFEDC Committee and are subject to correction by the author(s). The material does not necessarily reflect any position of the IFEDC Committee, its members. Papers presented at the Conference are subject to publication review by Professional Committee of Petroleum Engineering of Shaanxi Petroleum Society. Electronic reproduction, distribution, or storage of any part of this paper for commercial purposes without the written consent of Shaanxi Petroleum Society are prohibited. Permission to reproduce in print is restricted to an abstract of not more than 300 words; illustrations may not be copied. The abstract must contain conspicuous acknowledgment of IFEDC. Contact email: paper@ifedc.org.

© Springer Nature Singapore Pte Ltd. 2020

J. Lin (ed.), *Proceedings of the International Field Exploration and Development Conference 2018*, Springer Series in Geomechanics and Geoen지니어ing, https://doi.org/10.1007/978-981-13-7127-1_7

vibration acceleration might enhance the oil recovery in low permeable formation. Through matching four relative permeability models, a mechanism as enlarging the pore size distribution by vibration was verified further. It helped to substitute the capillary force test, which required a static measurement background and provided only experimental data of samples before or after vibration.

Keywords: Vibration acceleration · Water flooding · Relative permeability model · Pore size

1 Introduction

The crude oil price had decreased sharply in the last years, which hit the oil production seriously. In recent days, Corp. Petroteq had announced that BRPT was a low-cost technology for extremely shallow field to adapt to the serious background of low oil price. A key in this technology was that a physical wave field stimulated by artificial wave source was used. This news had made a surprise and might brought new vitality for technologies which were closely related to wave source. Two classical technologies utilizing wave during oil and gas field development process were seismic production technology and ultrasonic production technology. Seismic production technology used low-frequency wave, and ultrasonic production technology used high-frequency or ultrasonic wave. It had a substantial advantage in low wave attenuation and large operating range of 1–2 km.

Till now, seismic production technology had been used successfully in low permeability or heavy oil reservoirs of many fields. The mechanisms were verified with experiments, numerical studies, and field trials [1]. Besides the well-known mechanisms such as pressure supplement, permeability increase, and recovery enhancement, this technology was attractive as a physical method. It was environmental friendly and of low pollution to the reservoirs. Though there was a controversial statement worrying the damage to the cement, noise pollution, and minor effect, the unfavorable factors could be controlled after optimization of operating parameters. Especially, the low cost was very tempting and the harm was minor 50 m away from the source [2]. The experiments verified that seismic production technology improved oil recovery during water flooding through complex mechanisms [3, 4]. Though qualitative cognitions to the micromechanisms were obtained, the extent of influence of low-frequency vibration on rock property was not still clear.

For the object of optimization of operating parameters, quantitative study on the microvariation of rock properties should be done. A relation between the rock property variation and vibration parameters could be fitted through experiments or derived through dynamic mathematic analysis. Yan [5] analyzed the dimensionless relative flow velocity and porosity under different vibration frequency with capillary model. Sudo [6] and Shang [7] investigated the deformation of a drop under vibration in vertical direction and horizontal direction, respectively. Elkhoury [8] investigated the influence of pore pressure oscillations on the effective permeability of rocks fractured after placement in an experimental apparatus. An approximate semi-log relation was

found between normalized permeability increase and normalized pressure amplitude. The authors [9] also found a double-log relation between normalized permeability increase and solid displacement amplitude. Regardless of the specific values, a good agreement with the trend was achieved. Manga [10] reviewed the progress in changes in action distance, water level, and permeability. He also gave the mechanisms that enhance permeability as mobilization of particles, drops, and bubbles. Deng [11] presents a theoretical fluid dynamics model to describe how low-frequency elastic waves mobilize isolated droplets trapped in pores by capillary resistance. The ability of the theoretical model to predict the critical mobilization amplitudes and the displacement dynamics of the non-wetting droplet were validated. Karve [12, 13] outlined a systematic framework to assess the reliability of wave energy delivery to subsurface formations through numerical simulation.

The characteristics of low permeability rock during water flooding under low-frequency vibration were studied with experiments in this paper. A comparison of the absolute permeability at different water flooding stages before and after vibration was conducted. The relative permeability was got with unsteady-state technique. The fitting parameters in several classical functions about relative permeability were then derived, which explained indirectly the influence of low-frequency vibration on rock wettability and average pore radius. In the last, the variation of irreducible water saturation and the average pore radius was combined to describe the variation of capillary force curve under vibration. The analysis was used to provide a theoretical reference for mechanism explanation in seismic production technology.

2 Experiments and Results

2.1 Experimental Materials and Equipment

In the experiment, the simulated oil was a mixture of crude oil from Fengfuchuan oil field (79.9% saturates, 17.06% aromatics, 3.04% resins and asphaltenes) and kerosene with a proportion of 1:1. The viscosity of simulated oil at 30 °C was 28.8 mPa s. The simulated injection water was a solution of sodium chloride, calcium chloride, and magnesium chloride of mass concentration 70%: 12%: 18%. The simulated water was with a salinity of 40000 mg/L. The low permeable sand rocks were with similar gas permeability of $28 \times 10^{-3} \mu\text{m}^2$. The main instruments (Fig. 1) included a horizontal vibration table (made by Hai'an Oil Research instruments Co. Ltd., China), a core holder, and 2PB00C-type constant flux pump(Beijing Feisifurui Technology Ltd., China).

2.2 Experimental Procedure

(1) Method of absolute permeability under vibration

According to the conditions of oil reservoirs in Fengfuchuan oil field, the experiments were done at a constant temperature of 44 °C. The permeability of low permeable rock was measured at three times: end of water saturation k_{w1} , end of oil saturation (before and after vibration), and end of water flooding k_{w2} . After 8 h (no water flowed out) for oil saturation process, the oil permeability k_{oi} and irreducible water saturation S_{wci} were

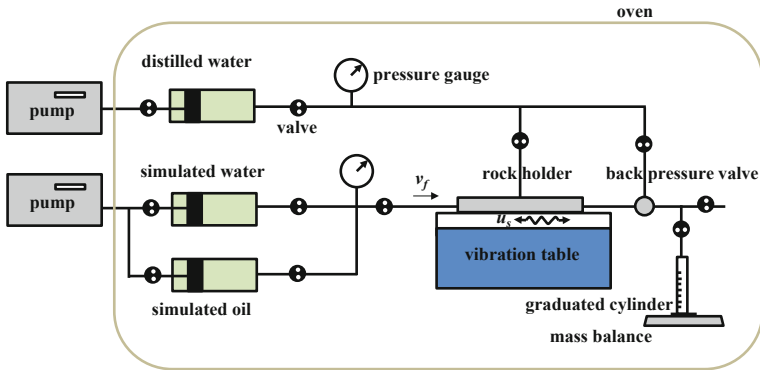


Fig. 1. Schematic diagram of water flooding under low-frequency vibration

measured. Then, the low-frequency wave stimulation of certain vibration parameters was activated until the end of the experiment. The direction of vibration was the same as the flow velocity. The operating frequency was chosen 20 Hz which was close to the natural frequency of matrix. Water was produced again under vibration. After 4 h (no water flowed out) for second oil saturation, the oil permeability k_{ov} and irreducible water saturation S_{wcv} were measured again. Through changing the vibration acceleration 0.1–0.6 m/s², the influence of vibration intensity on absolute permeability of low permeable rock during water flooding was conducted. The variation of irreducible water saturation was defined as $\nabla S_{wc} = 1 - S_{wcv}/S_{wci}$.

(2) Testing of relative permeability under vibration

During the water flooding process, the outputs of oil and water were recorded and used for calculation of relative permeability with unsteady-state technique. The saturation at equal-permeability point was got from the relative permeability curve. The residual oil saturations of rocks after water flooding under vibration S_{orv} or without vibration treatment S_{ori} as well as the equal-permeability point were calculated.

3 Variation of Rock Properties Under Vibration

The influence of low-frequency vibration acceleration on absolute permeability, relative permeability, displacement efficiency of low permeable rock in water flooding was got as below.

3.1 Changes in the Absolute Permeability

The absolute permeability during water flooding in low permeable rock was found to decrease with time. For example, the rock without vibration treatment had a water permeability of $18.04 \times 10^{-3} \mu\text{m}^2$ during water saturation, an oil permeability of $9.27 \times 10^{-3} \mu\text{m}^2$ after oil saturation, and a water permeability of $2.12 \times 10^{-3} \mu\text{m}^2$ at the end of water flooding. The decrease in pore pressure during water flooding and the

increase in stress sensitivity effect had caused the reduction in absolute permeability value [14, 15].

The ratios including k_{ov}/k_{oi} and k_{w2}/k_{w1} were used to demonstrate the influence of low-frequency vibration acceleration on absolute permeability. The ratio k_{ov}/k_{oi} reflected a direct effect of vibration on flow connectivity of rock. The ratio k_{w2}/k_{w1} reflected an indirect effect on retrieve of producing energy and decrease in stress sensitivity. The above ratios under different vibration acceleration are shown in Fig. 2.

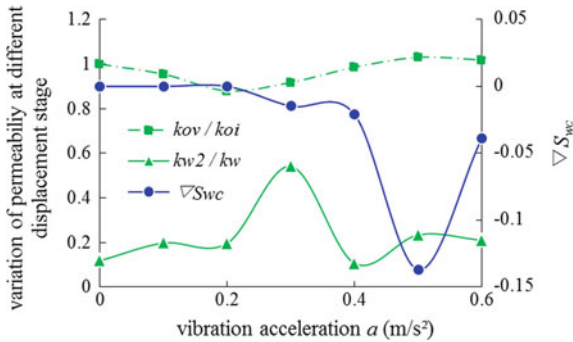


Fig. 2. Variation of absolute permeability and inducible water saturation under different vibration acceleration

Obvious fluctuation was found with both curves. Many papers had shown that artificial seismic could improve the permeability of the rock, especially around the natural frequency. However, the ratio k_{ov}/k_{oi} was lower than 1.0 when the acceleration was in the range 0.1–0.4 m/s², whereas the ratio was larger than 1.0 when the acceleration was larger than 0.4 m/s². When the vibration frequency was kept constant, the vibration amplitude indeed influenced the wave-induced cross-motion between solid and fluid. The cross-motion stimulated by sustained wave seemed to enhance the initial flow rate only when the vibration amplitude exceeded a certain value. There might exist a local optimal vibration amplitude to obtain the best enhancement of low connectivity in the low permeable rock saturated with low viscosity fluid. A stronger fluctuation inclined to cause desorption of liquid droplet from the rock surface. The isolated dispersing liquid droplet in the pore throats would also be carried out more easily by another displacement fluid, which can be verified by the variation of irreducible water saturation under vibration to some extent. The largest decrease in inducible water saturation (13.70%) and largest increase in absolute oil permeability (3.04%) were found at 0.5 m/s².

The phenomena indicated that both vibration amplitude and vibration frequency were important for proper effect of the artificial seismic production technology. The data of k_{w2}/k_{w1} shown the mechanism of artificial seismic production technology just as in other articles [16, 17]. The rock stimulated with vibration had a larger absolute permeability after water flooding in contrast to that without vibration treatment after water flooding. The indirect effect on retrieve of producing energy and decrease in

stress sensitivity was achieved. This ratio got a maximum value at 0.3 m/s^2 , which was different from that for k_{ov}/k_{oi} . The proper amplitude was suggested to be $0.3\text{--}0.5 \text{ m/s}^2$ to improve the whole flow conductivity combing the trends of k_{ov}/k_{oi} , k_{w2}/k_{w1} , and ∇S_{wc} .

3.2 Changes in the Relative Permeability

The influence of vibration on relative permeability was talked in some papers [18, 19]. The effects of lowering the inducible water saturation and residual oil saturation, increasing the oil permeability, as well as decreasing water permeability can also be found in Fig. 3. It was notable that the horizontal axis—water saturation S_w —was normalized. Though the rock samples were of same components as well as similar porosity and gas permeability, they had different irreducible water saturation and residual oil saturation without vibration because of the anisotropy and individual difference of the samples. The normalized water saturation for samples was defined as the product of water saturation without vibration treatment and $(1 - \nabla S_{wc})$.

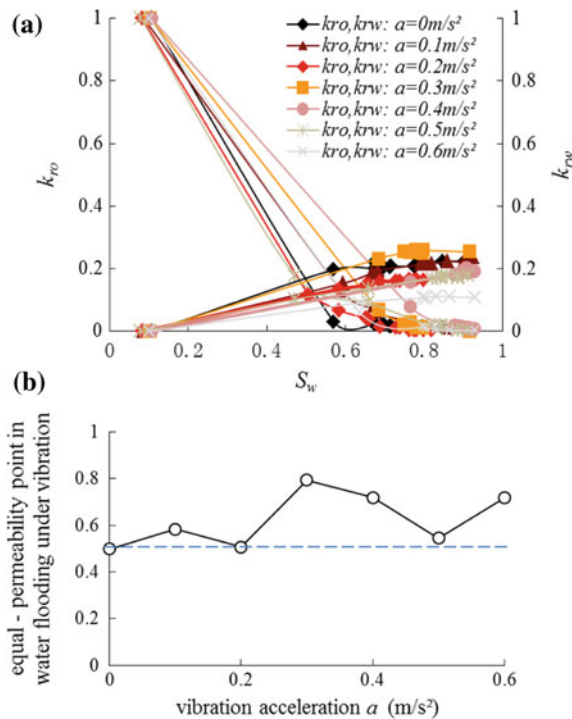


Fig. 3. The variation of relative permeability curve (a) and equal-permeability point (b) under vibration

The maximum decrement of water permeability and the maximum increment of oil permeability were found around the vibration acceleration of 0.3–0.4 m/s². Here, the oil/water permeability here referred to the relative permeability of a certain phase during water flooding. The oil/water permeability in Sect. 3.1 referred to the absolute permeability before or after water flooding, when one kind of fluid flowed mainly as a continuous phase. The isotonic points mainly move rightward under vibration. The variation of isotonic points meant that the hydrophilicity of rock was improved, which also verified the conclusion of other researchers [20, 21]. The vibration enhanced hydrophilicity of core achieved the highest increase under vibration acceleration of 0.3–0.4 m/s².

Though the mechanism of artificial seismic production technology as decreasing the inducible water saturation and connate oil saturation was talked, the trend of vibration amplitude versus connate oil saturation was scarcely shown. The variation of residual oil saturation under different acceleration ∇S_{or} in Fig. 4 was defined as Eq. 1 instead of $S_{orv}/S_{ori} - 1$. Though it was easy to make comparison between the irreducible water saturations under different vibration acceleration (measured before water flooding), the variation of residual oil saturation had to consider the influenced by the sample difference and various initial oil saturations.

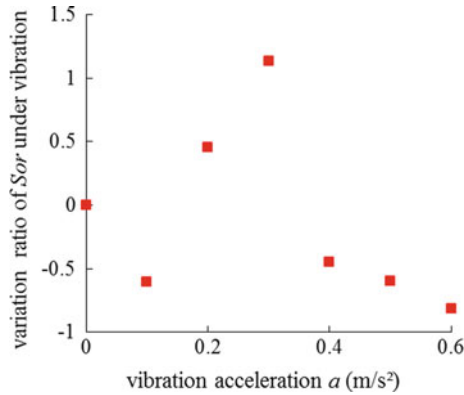


Fig. 4. Variation of residual oil saturation under different vibration acceleration

$$\nabla S_{or} = \frac{S_{orv}S_{wcv}}{S_{wci}S_{ori}} - 1 \quad (1)$$

Wherein ∇S_{or} is the variation of residual oil saturation under vibration; S_{orv} and S_{ori} are the residual oil saturations of rocks after water flooding under vibration or without vibration treatment, respectively; irreducible water saturation S_{wci} and S_{wcv} are the irreducible water saturation under vibration or without vibration treatment, respectively.

According to Eq. 1 and experimental data, ∇S_{or} was negative at most of the vibration accelerations. In addition, ∇S_{or} was found positive at 0.2 and 0.3 m/s^2 , where the maximum equal-permeability point and increment of oil relative permeability were achieved. The relation between proper vibration acceleration, residual oil saturation (negatively correlated with oil recovery), and wettability might be linked in low permeable sand rock under vibration. Anyway, it seemed that the residual oil saturation was prone to be decreased at violent vibration. As in Fig. 5 (left side), the main mechanisms of oil recovery enhancement of seismic production technology included detachment of a droplet from the soil surface and the droplet passing through a blocking throat successfully under a violent low-frequency vibration. The contact angle between oil phase and soil surface increased gradually to achieve a separation from the continuous phase. The decreases of residual oil saturation in Fig. 4 and in Fig. 2 inducible water saturation were mainly caused by these two mechanisms. Besides the increase in hydrophilicity, the decrease in oil viscosity had also enlarged the oil–water mobility ratio, which displaced water into smaller pore-throat and uniformed the waterflood front relatively. A strong vibration treatment was suggested in the field trial, and a negative effect might be caused by the artificial seismic production technology when an improper acceleration was set.

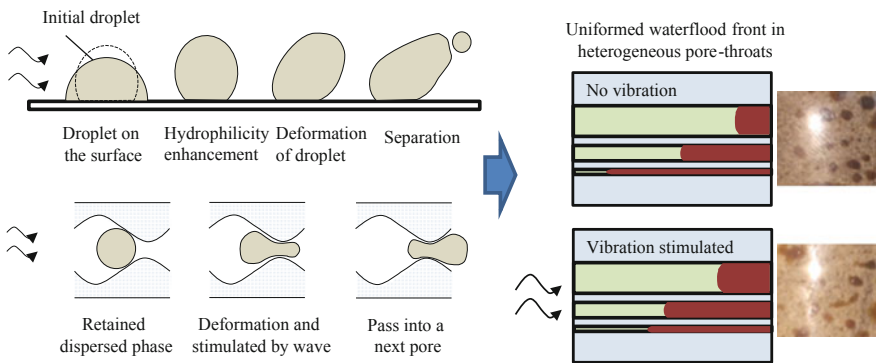


Fig. 5. The mechanism for oil recovery enhancement by vibration (droplet deformation and assisted displacement by wave)

4 Fitted Parameters About Relative Permeability and Pore Size Distribution

Laboratory determination methods of effective permeability and relative permeability included steady-state techniques, unsteady-state techniques, empirical techniques, and calculation from field data [22, 23]. The relative permeability curve in this paper was got through experiments with unsteady-state technique. In unsteady-state techniques, the production data were dealt, and a set of relative permeability curves were obtained using various mathematical methods, which were based on the Buckley–Leverett

equation for linear displacement of immiscible and incompressible fluids. Although the curves were got, a visible evaluation was only made with the variation of equal-permeability point, water or oil relative permeability. A deep discussion around the influence of low-frequency vibration on physical properties was needed. It may be conducted through curve match based on the empirical techniques such as Corey’s model and Land’s model.

Chen [24] and Ataie [25] listed several classic models which were widely used in reservoir engineering. Here, the functions including VGM, VGB, BCM, and BCB were referred in this paper to match the relative permeability curves.

In VG model, the functions of the capillary and permeability related to water saturation were in Eqs. 4–6. It was assumed that $m = 1 - 1/n$. The fitted parameters in VGM model and VGB model are both shown in Fig. 6. A proper assumption of $\eta = 0.5$ was based on the intermediate wettability of the rock without vibration treatment in Fig. 3, which was also given in Chen [24] in parameter optimization. The minor decrease in the values of n and m indicated that the width of pore size distribution seemed to increase generally with a large vibration acceleration. With a similar right value of main interval in pore size distribution (Fig. 7) before and after vibration in Yang [26], the probability distribution of large pore radius was increased. However, the width of pore size distribution at the acceleration 0.3 m/s^2 was smaller than that without vibration treatment.

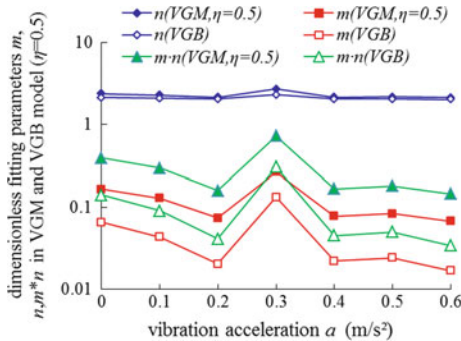


Fig. 6. The variation of fitted parameters in VG model under different vibration acceleration

Correspondingly, the probability distribution of large pore radius might have decreased to cause a high value of variation of residual oil saturation in Fig. 4. In addition, the fitted parameters in VGM model were a little larger than those in VGB model. The fitted parameters in both model had similar trend with vibration acceleration increasing. The values of m and $m \cdot n$ were in the range of 0.017–0.31 and in the range of 0.034–0.73, respectively, with the vibration acceleration 0–0.6 m/s².

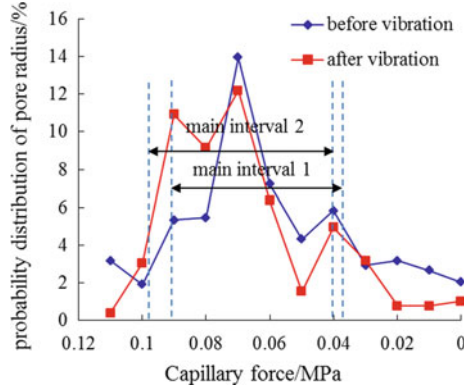


Fig. 7. The increase in width of pore size distribution and pore size after vibration in rock 4-1-1 in Yang [26]

$$\text{VG model, } S_{ew} = [1 + (\alpha_{vg} h_c)^n]^{-m} \tag{4}$$

$$\begin{aligned} \text{VGM model, } k_{rw} &= S_{ew}^\eta [1 - (1 - S_{ew}^{-m})^m]^2, \\ k_{ro} &= (1 - S_{ew})^\eta (1 - S_{ew}^{-m})^{2m} \end{aligned} \tag{5}$$

$$\begin{aligned} \text{VGB model, } k_{rw} &= S_{ew}^2 [1 - (1 - S_{ew}^{-m})^m], \\ k_{ro} &= (1 - S_{ew})^2 (1 - S_{ew}^{-m})^m \end{aligned} \tag{6}$$

Wherein S_{ew} is the normalized water saturation; h_c is capillary force height; α_{vg} is a fitting parameter inversely proportional to the non-wetting fluid entry pressure value; n is a fitting parameter inversely proportional to the width of pore size distribution; η is the tortuosity parameter.

In BC model, the functions of the capillary and permeability related to water saturation were in Eqs. 7–9. The fitted parameters in BC model are shown in Fig. 8.

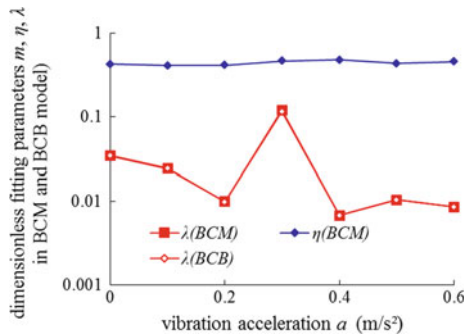


Fig. 8. The variation of fitted parameters in BC model under different vibration acceleration

$$\begin{aligned} \text{BC model, } S_{ew} &= (h_e/h_c)^\lambda, h_c > h_e; \\ S_{ew} &= 1, h_c \leq h_e \end{aligned} \quad (7)$$

$$\begin{aligned} \text{BCM model, } k_{rw} &= S_{ew}^{\eta+2+2/\lambda}; \\ k_{ro} &= (1 - S_{ew})^\eta \left(1 - S_{ew}^{1+1/\lambda}\right)^2 \end{aligned} \quad (8)$$

$$\begin{aligned} \text{BCB model, } k_{rw} &= S_{ew}^{3+2/\lambda}; \\ k_{ro} &= (1 - S_{ew})^2 \left(1 - S_{ew}^{1+2/\lambda}\right) \end{aligned} \quad (9)$$

Wherein h_e equaled to the non-wetting fluid entry pressure; λ is the characteristic soil parameter, characterizing the pore size distribution.

The fitted value of λ under certain vibration acceleration in BCM model was almost same with that in BCB model. It decreased generally with violent vibration. The VG model was asymptotically equaled to the BC model in the dry range when h_c becomes large, $S_{ew} = [(1 - \alpha)/h_c]^m$, such that $1 - \alpha = h_e$ and $\lambda = m \cdot n$. Because the experimental rock was low permeable, the capillary force was large enough. A similar trend of λ in Fig. 6 with $m \cdot n$ was observed successfully. Certainly, the fitted values of λ , were in the range of 0.006–0.11 and lower than $m \cdot n$. The tortuosity parameter had increased from 0.42 to 0.48 under vibration, which indicated that $\eta = 0.5$ in Fig. 6 was properly assumed. The largest value of η was found with 0.3–0.4 m/s².

The mechanisms about seismic production technology had shown that the properties of fluid and rock grain would be a little influenced by low-frequency vibration. Especially, the property of fluid would basically return to its initial value after stopping vibration for a certain time. When α_{vg} was assumed to keep constant under low-frequency vibration, the variation of n would only lead to a minor change of α_{vg} as well. The minor decrease in m or λ (less than 1.0) would cause the generalized water saturation to increase according to Eqs. 4 and 7. Thereby, the saturation of non-wetting phase was increased when the capillary force curve of rock sample was measured quickly after vibration treatment.

5 Conclusions

The properties of rock were affected under the stimulation of artificial seismic production technology, which might improve the injection or production in actual sand reservoir. The influence of low-frequency vibration acceleration on variation trend of properties of low permeable rock during water flooding was studied through experiments and further discussion. The main results can be summarized as follows:

- (1) It was observed that amounts of the properties during water flooding in a low permeable rock, including conductivity of rock, relative permeability of oil–water phase and oil recovery, were changed under vibration. As the displacement

proceeded, the conductivity gradually decreased due to the stress sensitivity, but this degree of variation was degraded by vibration.

- (2) The hydrophilicity of rock was enhanced by vibration, which was indicated from the rightward movement of equal-permeability point, to make the water pass through more throats and to detach more oil droplet from the soil surface. Thereby, the relative permeability of water phase was decreased, and the relative permeability of oil phase was increased.
- (3) It was concluded that a violent vibration was proper for artificial seismic production technology because of the largest decrease in inducible water saturation and residual oil saturation, as well as the largest improvement in water displacement efficiency. The increased width of pore size distribution under vibration, which was got from relative permeability curve matching, might play a role for above improvement.

Acknowledgements. This study was supported by the China Postdoctoral Science Foundation (2018M631765), a grant from Hebei Province Postdoctoral Advanced Programs (B2018003011), Scientific and Technological Research Project of Higher Education Institutions in Hebei Province (QN2019163), and the Doctoral Funds of Yanshan University (BL17024).

References

1. Uetani Takaaki, Matsuoka Toshifumi, Honda Hiromi. Investigation of the conditions required for improved oil recovery by an earthquake. *SPE Prod Oper.* 2016;31(3):219–27.
2. Yu HL. Experimental study on increase of oil yield by means of artificial ground shaking for an oil pool in Inner Mongolia. *Earthquake Eng Eng Vibr.* 2000;20(4):148–53.
3. Ariadji T. Effect of vibration on rock and fluid properties: on seeking the vibroseismic technology mechanisms, In: *SPE Asia Pacific oil and gas conference and exhibition*, Jakarta, Indonesia, April 2005, pp. 1–8.
4. Kurawle I, Kaul M, Mahalle N, et al. Seismic EOR—the optimization of aging waterflood reservoirs. *Offshore Europe: Aberdeen, UK*, September; 2009. p. 1–5.
5. Yan P. Reservoir analysis using intermediate frequency excitation. Ph.D. Thesis, Stanford University, 1999.
6. Sudo S, Goto A, Kuwano H, et al. The dynamic behavior of liquid droplets on vibrating plate. *J JSEM.* 2010;10:38–45.
7. Shang XS, Pu CS, Yu GL, et al. Study on micro-dynamic mechanism of droplet motion under vibration. *Sci Technol Eng.* 2013;13(8):2166–9.
8. Elkhoury JE, Niemeijer A, Brodsky EE, et al. Laboratory observations of permeability enhancement by fluid pressure oscillation of in-situ fractured rock. *J Geophys Res Solid Earth.* 2011;116(B2):1–15.
9. Zheng LM, Pu CS, Liu J. Influence of low-frequency vibration oil recovery on the initial flow of radial reservoir. *Petrol Geol Recovery Effi.* 2018;25(1):68–76.
10. Manga M, Beresnev I, Brodsky EE, et al. Changes in permeability caused by transient stresses: Field observations, experiments, and mechanisms. *Rev Geophys.* 2012;50(2):1–24.
11. Deng W, Cardenas MB. Dynamics and dislodgment from pore constrictions of a trapped non wetting droplet stimulated by seismic waves. *Water Resour Res.* 2013;49:4206–18.

12. Karve PM, Kucukcoban S, Kallivokas LF. On an inverse source problem for enhanced oil recovery by wave motion maximization in reservoirs. *Comput Geosci*. 2015;19:233–56.
13. Karve PM, Kallivokas LF, Manuel L. A framework for assessing the uncertainty in wave energy delivery to targeted subsurface formations. *J Appl Geophys*. 2016;125:26–36.
14. Li S, Tang DZ, Pan ZJ, et al. Characterization of the stress sensitivity of pores for different rank coals by nuclear magnetic resonance. *Fuel*. 2013;111:746–54.
15. Geng YG, Tang DZ, Xu H, et al. Experimental study on permeability stress sensitivity of reconstituted granular coal with different lithotypes. *Fuel*. 2017;202:12–22.
16. Belonenko VN. Vibro seismic technology for increasing hydrocarbon bed recovery”, *New Technologies for the 21st Century, Joint English/Russian Magazine*, 2000, 4, p. 14.
17. Cidoncha JG. Application of acoustic waves for reservoir stimulation In: *International oil conference and exhibition in Mexico, Veracruz, Mexico, June 2007*, pp. 1–7.
18. Nikolaevskiy VN, Lopukhov GP, Liao YZ, et al. Residual oil reservoir recovery with seismic vibrations. *SPE Prod Facil*. 1996;11(2):89–94.
19. Liu J, Pu CS, Lin CY, et al. Effect of low-frequency vibration on a relative permeability curve and irreducible water saturation. In: *International conference on artificial intelligence and industrial application, Hangkang, China, January 2015*, pp. 889–896.
20. Li MY, Dong ZX, Ji SL, et al. Sound vibration on wettability of rock surface. *Acta Petrolei Sinica*. 1999;20(6):57–62.
21. Sun RY, Cheng GX. Effect of artificial vibration on liquids flow through porous media. *J Hydrodyn*. 2004;19(4):552–7.
22. Krause MH, Benson SM. Accurate determination of characteristic relative permeability curves. *Adv Water Resour*. 2015;83:376–88.
23. Kianinejad A, Chen XY, DiCarlo DA. Direct measurement of relative permeability in rocks from unsteady-state saturation profiles. *Adv Water Resour*. 2016;94:1–10.
24. Chen J, Hopmans JW, Grismer ME. Parameter estimation of two-fluid capillary pressure–saturation and permeability functions. *Adv Water Resour*. 1999;22(5):479–93.
25. Ataie-Ashtiani B, Raeesi-Ardekani D. Comparison of numerical formulations for two-phase flow in Porous Media. *Geotech Geol Eng*. 2010;28:373–89.
26. Yang L, Ma JG, Wei RL, et al. The effects of mechanical vibration on the capillary pressure curve and the wettability of a core. *J. Xi’an Petrol Inst* 1997;12(5):23–25, 35.